Technoeconomic optimisation and comparative environmental impact evaluation of continuous crystallisation and antisolvent selection for artemisinin recovery

Computers and Chemical Engineering 103 (2017) 218–232

Contents lists available at ScienceDirect

Computers and Chemical Engineering

journal homepage: www.elsevier.com/locate/compchemeng

Technoeconomic optimisation and comparative environmental impact evaluation of continuous crystallisation and antisolvent selection for artemisinin recovery

Hikaru G. Jolliffe, Dimitrios I. Gerogiorgis *

Institute for Materials and Processes (IMP), School of Engineering, University of Edinburgh, The King's Buildings, Edinburgh EH9 3FB, United Kingdom

ARTICLE INFO

Article history:
Received 5 December 2016
Received in revised form 20 February 2017
Accepted 25 February 2017
Available online 28 February 2017

Keywords:
Continuous Pharmaceutical Manufacturing (CPM)
Nonlinear Programming (NLP)
Optimisation
Crystallisation
Solvent selection
Artemisinin

ABSTRACT

Systematic nonlinear optimisation is a valuable tool towards evaluating the performance of conceptual Continuous Pharmaceutical Manufacturing (CPM) flowsheets. This study considers total cost minimisation of multiple plausible design choices and eight candidate antisolvents for the continuous recovery of artemisinin (a potent antimalarial Active Pharmaceutical Ingredient/API) via continuous crystallisation, with simultaneous evaluation of process mass and environmental efficiency via the *E*-factor (an established green chemistry metric). Essential design variables include the crystallisation cooling temperature, the antisolvent requirements and the use of multiple crystallisers in series. Acetonitrile achieves the minimum total cost for one crystalliser ($761 \cdot 10^3$ GBP, for a crystallisation at 5 °C, with 80% antisolvent addition and an *E*-factor of 29.1). The use of a second crystalliser in series allows for further total cost savings for all antisolvents; *E*-factors continue to decrease accordingly, albeit with very limited scope for each successive crystalliser due to negligible productivity improvements.

1. Introduction

Growing R&D expenditure, increasing competition from generic manufacturers and financial pressures on the pharmaceutical industry (Fig. 1) have led to the emergence of Continuous Pharmaceutical Manufacturing (CPM) as a promising alternative to the current paradigm of batch production (Gutmann et al., 2015). While possessing significant benefits including equipment flexibility and extensive industrial know-how of a mature technology, batch manufacturing is hampered by remarkable disadvantages, including low efficiency (of both material and energy use), problematic process scale-up and poor heat and mass transfer. The methodologies for CPM are exceptionally beneficial towards ensuring Quality by Design (QbD), which has been fully adopted as a strategic priority by the U.S. pharmaceutical industry; moreover, they are closely related to the significant instrumentation and algorithmic advances in Process Analytical Technology (PAT), which enables unprecedented data acquisition and insight into pharmaceutical process monitoring and control. Consequently, the current groundbreaking developments in articulating the concepts and exploring the boundaries of CPM, QbD and PAT have the strongest approval of the most influential and authoritative regulatory bodies (Lee et al., 2015).

Artemisinin is one of the most important antimalarial substances available today. First identified and isolated from the plant *Artemisia annua* in the late 1970s (Tu, 2011), an accomplishment for which the 2015 Nobel Prize in Physiology or Medicine has been awarded, artemisinin is currently produced via batch extraction from the cultivated plant (Fig. 2). However, long product lead times and fluctuating demand due to the unpredictable burden and outbreaks of malaria lead to highly variable prices and production levels (Jolliffe and Gerogiorgis, 2016a). Recent research has demonstrated the continuous synthesis of artemisinin (Kopetzki et al., 2013; Seeberger et al., 2014). This novel synthesis route uses a waste product from the current batch production process as a feedstock, and produces artemisinin via two sequential plug flow reactors (PFRs), the first of which employs photo-oxidation. High API product yields can be achieved, and the process has been further adapted to produce several artemisinin derivatives (Gilmore et al., 2014).

In recent years the continuous synthesis of a range of APIs has been demonstrated, from common over-the-counter medications to key anti-cancer drugs (Bana et al., 2016). However, while significant advances have been achieved in sophisticated microscale flow reactor technology, continuous separation technologies which are also essential to combine with the former are still only

* Corresponding author. Tel.: +44 131 6517072.
E-mail address: D.Gerogiorgis@ed.ac.uk (D.I. Gerogiorgis).

http://dx.doi.org/10.1016/j.compchemeng.2017.02.046
0098-1354/

Nomenclature and acronyms

API	active pharmaceutical ingredient
A_{COBC}	internal surface area of the COBC, m^2
BLIC	Battery Limits Installed Cost of all equipment in a process, part of *CapEx*, £
CapEx	capital expenditure, £
C_{mi}	concentration of species *i* in reactor *m*, mol L^{-1}
C_{mi0}	initial concentration of species *i* in reactor *m*, mol L^{-1}
$C_{P,AS}$	heat capacity of antisolvent, J $kg^{-1}K^{-1-1}$
$C_{P,CW}$	heat capacity of cooling fluid, J $kg^{-1}K^{-1}$
$C_{P,Tol}$	heat capacity of toluene, J $kg^{-1}K^{-1}$ continuous pharmaceutical manufacturing
COBC	continuous oscillatory baffled reactor
$Cost_{Tot}$	total cost, the total costs over a certain plant lifetime, adjusted to the present, £ battery-limits-installed-cost
CPM	Continuous Pharmaceutical Manufacturing
f_{con}	factor relating the contingency to the Battery-Limits-Installed-Cost
f_{Crys}	factor to account for non-attainment of equilibrium in the COBC
$f_{\gamma i}$	summary of factors used in Eq. (16)
FOB_{Tot}	(total) Free-On-Board cost of equipment
f_{utl}	factor relating the cost of utilities to the total annual requirements (kg) of material
f_{was}	factor relating the cost of waste handling to the volume of waste
f_{wc}	factor relating the working capital to the cost of materials
k_{mi}	rate constant of species *i*, reactor *m*, L mol^{-1} hr^{-1} m^{-1}
LMTD	log mean temperature difference
$\dot{m}_{API,prod}$	mass of API produced after separation, kg yr^{-1}
$\dot{m}_{AS}$	mass flow of antisolvent in the COBC, g hr^{-1}
m_{BPD}	mass of by-product waste, kg yr^{-1}
$m_{Crys,API,0}$	initial mole fraction of API in the COBCr
$m_{Crys,API,f}$	final mole fraction of API in the COBCr
$\dot{m}_{CW}$	cooling fluid requirement, kg s^{-1}
$\dot{m}_{Tol}$	mass flow of toluene in the COBC, g hr^{-1}
m_{UAPI}	mass of unrecovered API, kg yr^{-1} temperature, °C or K
m_{ur}	mass of unreacted reagent waste, kg yr^{-1}
m_{WAS}	total mass of waste, kg yr^{-1}
m_{WS}	mass of solvent waste, kg yr^{-1} m
$n_{AS,COBC}$	molar flow of antisolvent in the COBC, mol hr^{-1}
n_i	number (quantity) of equipment *i*
$n_{Tol,COBC}$	molar flow of toluene in the COBC, mol hr^{-1}
OpEx	operating expenditure, £
p_i	exponent used in Eq. (16)
Q_m	flowrate through reactor *m*, mL hr^{-1}
q_{COBC}	cooling duty in COBC, W
$R^T{}_{Crys}$	theoretical API recovery in the COBC at equilibrium
R_{Crys}	API recovery in the COBC
r_{mi}	reaction rate of molecule *i* in reactor *m*, mol L^{-1} hr^{-1}
R_i	annual requirements of material *j*, kg y^{-1}
S_{ai}	reference capacity of item *i*, units depend on item type
S_{bi}	design capacity of item *i*, units depend on item type
T	temperature, °C or K^{-1}
T_{Crys}	temperature of crystallisation, °C
$T_{Crys,LO}$	cooling target temperature of crystallisation, °C
U_{COBC}	overall heat transfer coefficient of the COBC, W m^{-2} K^{-1}
V_{PFRm}	volume of plug flor reactor *m*, mL
$x_{API,Crys}$	mole fraction of API in the crystalliser
x_{ki}	mole fraction of species *i* in stream *k*
X_{mi}	conversion of species *i* in PFR *m*
X_{mif}	Final conversion of species *i* in PFR
y	discount rate, the correction factor for adjusting costs to the present
α_0	Coefficient used in Eq. (9)
α_1	Coefficient used in Eq. (9)
α_2	Coefficient used in Eq. (9)
ΔT_{COBC}	Temperature change from the cooling inside the COBC
γ_{ai}	reference cost of item *i*
γ_{cont}	cost of contingency, £
γ_{ec}	factor to account for equipment engineering and construction
γ_{ins}	factor to account for equipment installation
γ_{ins2}	factor to account for equipment instrumentation
γ_{mat}	cost of material raw material purchase (including solvents and catalysts), £
γ_{pip}	factor to account for equipment piping
γ_{utl}	cost of utilities, £
γ_{was}	cost of waste handling, £
γ_{wc}	cost of working capital, £
$\dot{v}_{was}$	annual generation of waste, L y^{-1}
π_j	price of material *j*, £ kg^{-1}
τ	plant lifetime, years

gradually becoming available (Heider et al., 2014; Baxendale et al., 2015; Jensen, 2017).

Process synthesis, first-principles modelling, simulation and cost estimation are extremely valuable methodologies for evaluating the benefits of continuous processing in pharmaceutical production (Gerogiorgis and Barton, 2009; Jolliffe and Gerogiorgis, 2016a,b,c, 2017; Diab and Gerogiorgis, 2017). Furthermore, systematic model-based optimisation has also been successfully used in many CPM design and operation case studies (Gernaey et al., 2012; Escotet-Espinoza et al., 2016). A relevant publication explored the optimisation of continuous production campaigns (Sahlodin and Barton, 2015). After studying the suitability of existing optimisation methods for continuous production lines, a novel approach has been proposed whereby the objective function is the maximisation of on-spec product, as opposed to the minimisation of start-up/shut-down time which is commonly used in higher-volume sectors. A significant contribution of the new approach is that it can be efficiently combined with gradient-based methods, due to the differentiability of the formulations proposed.

A recent study addressed reaction parameter estimation for a challenging continuous flow synthesis case: a nonlinear regression problem (with over 15 chemical species, 27 reactions and 29 parameters) has been formulated and solved for the optimisation of Lorcaserin synthesis, covering several key aspects of CPM design and optimisation techniques (Grom et al., 2016). Therein, the efficient use of the Levenberg-Marquardt algorithm enabled a computationally efficient global optimisation. Another successful implementation of systematic process systems engineering methods in the field of CPM is the optimisation of lab-scale continuous ibuprofen synthesis, with a focus on microreactor design and operation, mass and energy balances, reaction rates and reactor configurations (Patel et al., 2011); this study did not consider API product separation, but presented a novel formulation for the model-based minimisation of the difference between heat flow to and from the continuous flow reactor.

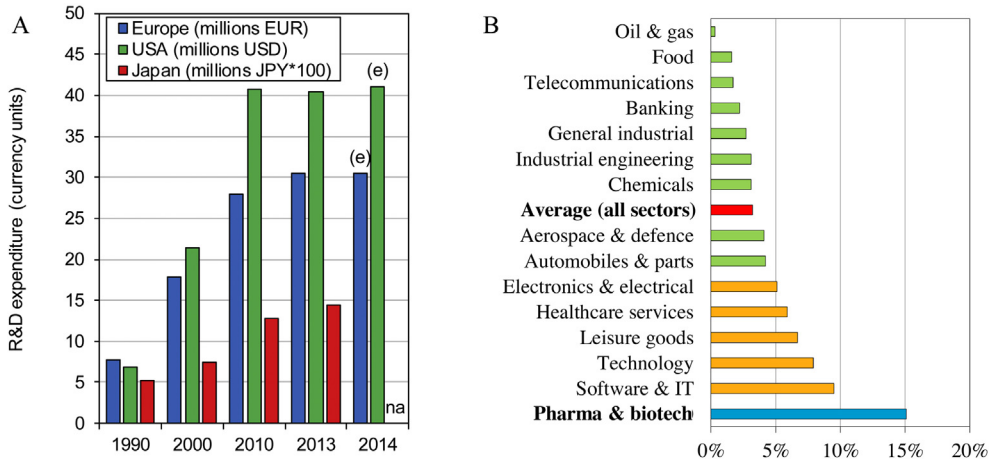

Fig. 1. Economic and market pressures faced by the pharmaceutical industry. (A) Typical R&D and marketing costs for a high-volume (blockbuster) pharmaceutical product. (B) R&D costs of various industrial sectors as a percentage of total sales. (EFPIA, 2013).

Fig. 2. Artemisinin is extracted from the plant *Artemisia annua*, and is often used in medical formulations known as Artemisinin Combination Therapies (ACTs). Adapted from PATH (2016).

Continuous downstream pharmaceutical processes have also attracted strong research interest with respect to optimisation and control (Ierapetritou et al., 2016; Haas et al., 2017). Surrogate modelling can address black-box feasibility problems: Wang and Ierapetritou (2017) propose a Radial Basis Function (RBF)-based method, expanding on previous work in which kriging has been used to accurately determine feasible region boundaries (Boukouvala and Ierapetritou, 2013; Rogers and Ierapetritou, 2015a,b). The proposed RBF method, which uses adaptive sampling, can efficiently sample regions of high prediction uncertainty: in all cases studied, the RBF method outperforms the previously developed kriging-based method (Wang and Ierapetritou, 2017).

Monte Carlo methods have also been use to model, predict and control crystallisation, in both stirred-tank (Kwon et al., 2014a) and plug-flow crystallisers (Kwon et al., 2014b). Protein crystal nucleation, growth and dissolution have been modelled via the use of kinetic Monte Carlo (kMC) simulations, which are combined with population balance equations towards describing the evolution and behaviour of crystal distributions within crystalliser vessels. Kwon et al. (2014a,b) have successfully developed a model-predictive (MPC) controller to manipulate vessel jacket temperature; furthermore, they have determined the optimal superficial velocity and proposed a novel MPC control strategy to handle disturbances in feed flow, thus ensuring high-performance plug flow crystalliser operation (Kwon et al., 2014b).

Further case studies have also focused on the detailed modelling and optimisation of downstream pharmaceutical processes, such as tablet formation. By considering a hybrid model-predictive control (MPC) model for moving horizon-based optimisation, Singh et al. (2015) achieved profit maximisation for a continuous tablet formation process which adheres to QbD principles. Furthermore, nanofiltration membrane cascades for solvent recovery in continuous pharmaceutical processes has been expored via a nonlinear optimisation formulation implemented in GAMS® (Abejón et al., 2014, 2015): according to this study, total costs can indeed be significantly reduced by implementing continuous solvent recovery.

Life Cycle Assessment (LCA) studies for novel CPM processes have employed optimisation methods as a core component of relevant analyses (Ott et al., 2014). Systematic optimisation encompassing the consideration of a wide range of performance criteria enables more advantageous process design and operation, allowing for a reduction in Life Cycle Impact Assessment (LCIA) scores by up to 45% (Ott et al., 2016). Nevertheless, the emergence of novel pharmaceutical technologies also illustrates the pressing need for method standardisation in order to address data gaps, as well as the importance of consistent sensitivity analyses (Kralisch et al., 2014).

Continuous product separation and crystallisation are key unit operations in the drive towards realizing the robust and efficient implementation of CPM. Our previous studies have explored the potential performance of eight candidate antisolvents for continuous crystallisation of artemisinin via detailed process simulation, using both predicted and experimentally reported API solubilities (Jolliffe and Gerogiorgis, 2016a,b). Furthermore, we have previously employed nonlinear optimisation towards identifying ideal continuous separation designs for ibuprofen: the preferred temperature, solvent and liquid–liquid extraction configuration – towards which achieve the minimum total cost for a CPM process – have been determined via comprehensively considering plantwide mass and molar balances, explicit reaction kinetics, parameter estimation, mass transfer, thermodynamics and economic modelling (Jolliffe and Gerogiorgis, 2017).

The present study focuses on further investigating the continuous separation of artemisinin by formulating a Nonlinear Programming (NLP) optimisation problem which simultaneously

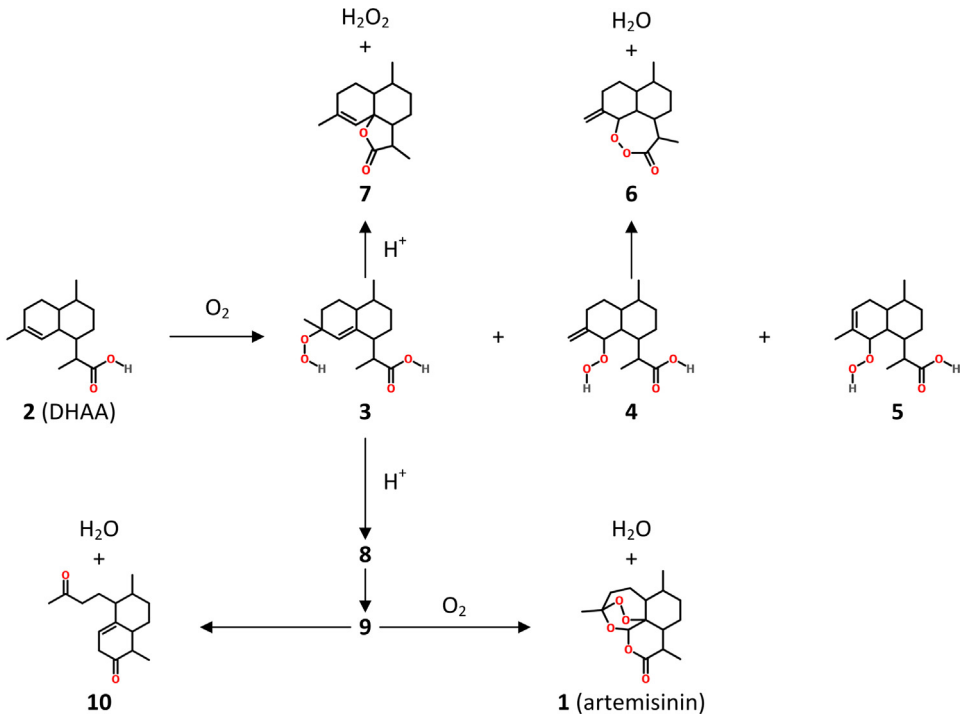

Fig. 3. Reaction sequence used by Kopetzki et al. (2013) for continuous artemisinin synthesis.

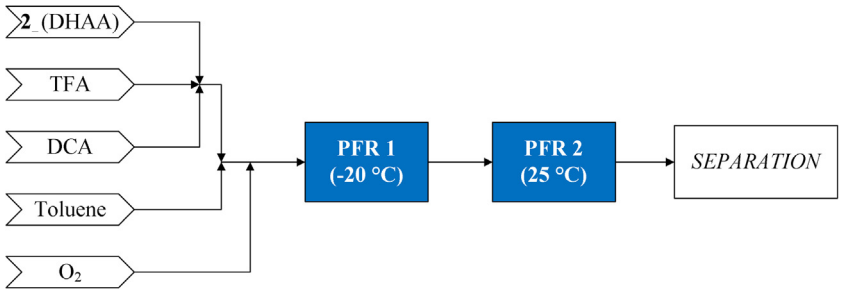

Fig. 4. Demonstrated process flowsheet for the continuous production of artemisinin (Kopetzki et al., 2013).

considers process modelling, API solubility prediction via group contribution methods (UNIFAC), and environmental and sustainability metrics (namely the *E*-factor), for several candidate API crystallisation antisolvents. The CPM process studied here is based on the continuous flow synthesis chemistry developed recently for artemisinin (Kopetzki et al., 2013), which already has been shown to be compatible with a range of separation methods (Horváth et al., 2015).

The paper is structured as follows: first, the continuous flow synthesis chemistry is presented. Secondly, the continuous separation of the API product is discussed, summarising previous contributions and illustrating how those results are used in the context of the present research objective. This is followed by the formulation of the nonlinear optimisation problem, and the detailed development of the objective function the key equations encompassing process modelling, product separation and economics, the necessary problem constraints, and the corresponding MATLAB® code structure. The presentation of computational results follows, with a detailed discussion of the emerging trends and their implications for technical feasibility, economic viability and environmental impact of the CPM plant design options evaluated.

2. Process flowsheet and continuous API product separation

Numerous publications document the significant research effort in recent years towards producing both synthetic and semi-synthetic artemisinin (Paddon et al., 2013; Amara et al., 2015). The continuous synthesis route studied here is one of particular interest, recently demonstrated by Kopetzki et al. (2013). Dihydroartemisinic acid (DHAA, **2**) – currently routinely discarded as waste – is transformed via intermediates to artemisinin using photo-oxidation with subsequent acid catalysis (Fig. 3). There are plans to commercialise this process, which has been extended to produce various artemisinin derivatives (Gilmore et al., 2014).

2.1. Reaction system

The flowsheet (Fig. 4) is based on a recent proven continuous synthesis route (Fig. 3) (Kopetzki et al., 2013). Two plug flow reactors are employed. In the first, the key ingredient DHAA (**2**) undergoes chilled photo-oxidation at −20 °C: it is subjected to a monochrome light source and the addition of the photosensitising dye, 9,10-dicyanoanthracene (DCA), which promotes the genera-

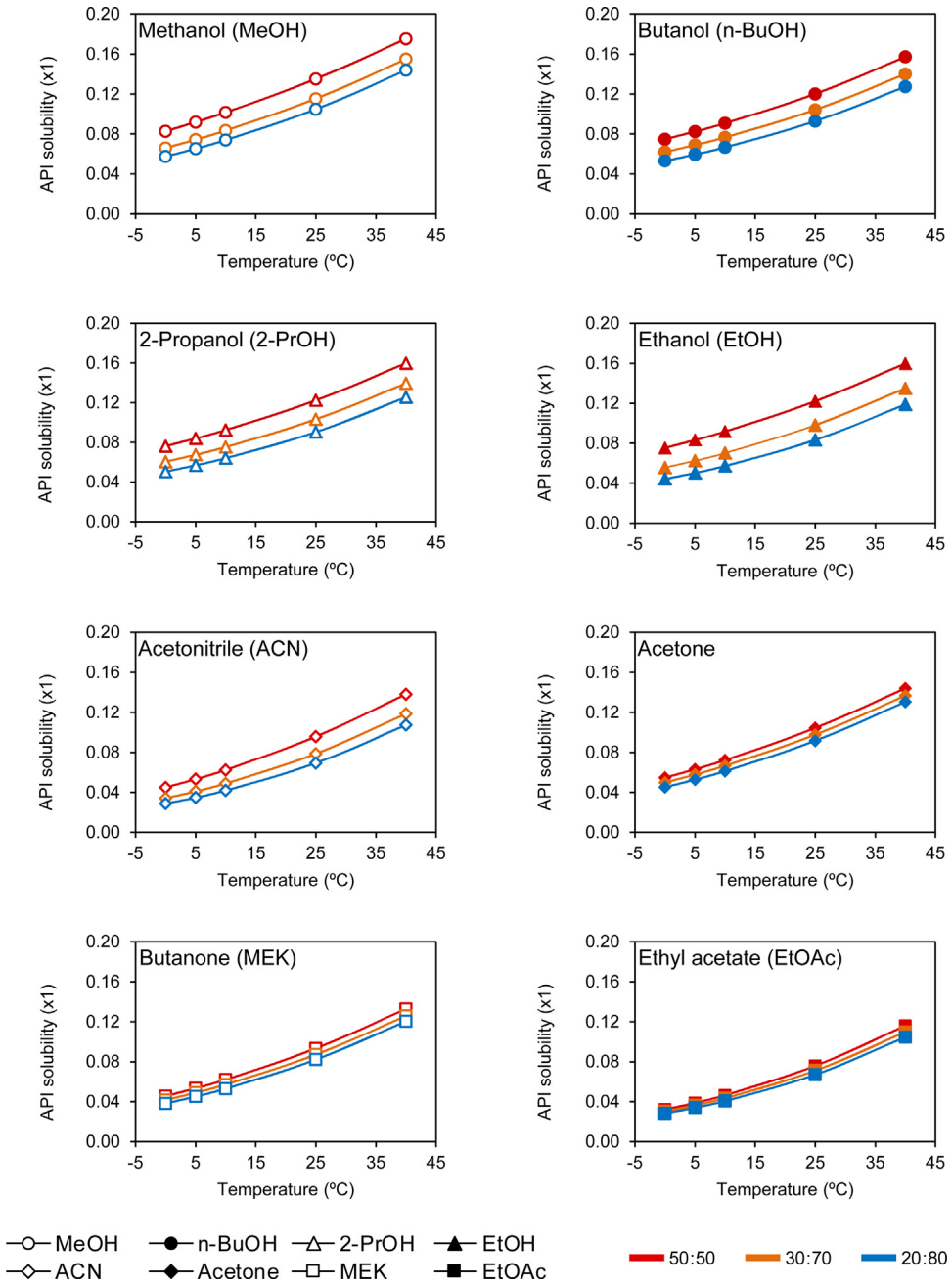

Fig. 5. Artemisinin solubility evaluation for eight candidate continuous crystallisation antisolvents, using the UNIFAC activity coefficient prediction method. Candidate antisolvents appear in order of decreasing API solubility. The vertical axis is in mole fraction units (Jolliffe and Gerogiorgis, 2016a).

tion of singlet oxygen. The products are key intermediate **3** and by-products **4** and **5** (Kopetzki et al., 2013).

In the second reactor, several reactions occur simultaneously. The key reaction sequence transforms intermediate **3** into **9** via a Hock rearrangement, by the action of an acid catalyst (trifluoroacetic acid, TFA); intermediate **9** then further undergoes oxidation with triplet oxygen to produce the API product, artemisinin (species **1**). Other reactions occur as well, leading to further by-products (species **6** and **10**) (Kopetzki et al., 2013; Gilmore et al., 2014).

PFR reactor design requires the calculation of the process mass balances. Examples of relevant artemisinin CPM process mass balances at different production scales have been reported in our recent publications (Jolliffe and Gerogiorgis, 2016a,b,c), which have also been based on the continuous flow synthesis chemistry studied here. Essential process modelling assumptions in order to determine plantwide mass balances prescribe that reactions occur only inside the PFR reactors and not in any connecting process lines, isothermal operation is ensured in all PFR reactors via sufficient heat transfer, there is no phase transformation or precipitation affecting the flow, and oxidising gas stream (oxygen) to liquid process solvent (toluene) mass transfer does not limit the efficiency of the artemisinin synthesis reaction.

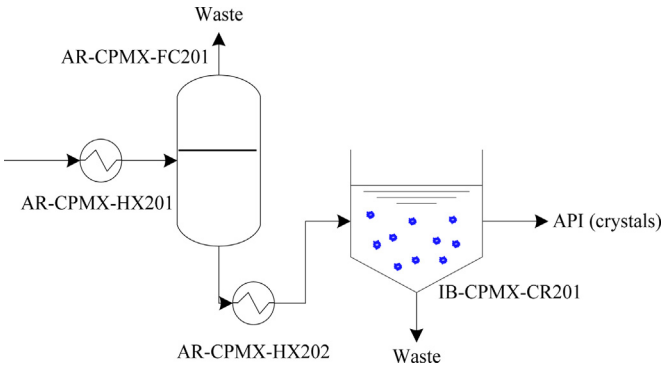

Fig. 6. Conceptual flowsheet for continuous artemisinin separation via crystallisation. After API product stream concentration via solvent evaporation, a continuous (here, a CSTR-type) crystalliser is employed.

2.2. Continuous API product separation

A recent paper has illustrated the implementation of process modelling and simulation for the use of the antisolvents studied here in continuous pharmaceutical manufacturing (Jolliffe and Gerogiorgis, 2016a). Eight common solvents have been investigated as potential antisolvents for use in continuous artemisinin crystallisation: ethanol (EtOH), acetone, ethyl acetate (EtOAc), methanol (MeOH), 2-propanol (2-PrOH), n-butanol (n-BuOH), butanone (methyl-ethyl ketone, MEK) and acetonitrile (ACN). Artemisinin solubilities have been computationally evaluated for the temperature range between 0 and 40 °C, for toluene-to-antisolvent ratios of 50:50, 30:70, and 20:80 by weight (Fig. 5). A generalised conceptual flowsheet of the continuous separation system design is presented in Fig. 6.

Further CPM process simulations performed under slightly different assumptions (regarding unit operation selection and material requirements) illustrate the considerably varying performance of these candidate continuous crystallisation antisolvents (Jolliffe and Gerogiorgis, 2016b) (Figs. 7 and 8). Ethyl acetate and acetonitrile are promising antisolvents, while methanol and butanol suggest significantly inferior performance. Based on the model employed by Jolliffe and Gerogiorgis (2016b), most of these antisolvents follow a similar trend of improving mass efficiency (*E*-factor) with greater API recovery, with certain exceptions (Fig. 8). There is an apparent limit to the minimum environmental impact (lowest *E*-factor) that can be attained for this conceptual continuous API separation process.

These eight antisolvents have been revisited in the present technoeconomic optimisation analysis, having been integrated into a more elaborate nonlinear total cost minimisation problem formulation, which again relies on our previously published API solubility estimations. Prior to the crystallisation operation, some solvent removal is assumed to occur, as a higher raw feed stream API concentration is required to ensure continuous crystallisation feasibility (Horváth et al., 2015). Furthermore, impurities are assumed to not co-crystallise with the API product.

2.3. Continuous Oscillatory Baffled Crystalliser (COBC)

Crystallisation via solution cooling is a commonly used unit operation in many industries, including fine chemicals and pharmaceuticals. Crucial process parameters towards efficient purification and control over API crystal size distribution, morphology, and purity are heat and mass transfer, and these become even more important with the very high purity requirements and stringent quality specifications which are quintessential for pharmaceuticals (Su et al., 2015).

A remarkable recent development in crystalliser technology is the Continuous Oscillatory Baffled Crystalliser (COBC). Developed on the basis of COB reactor technology, it combines the benefits of plug flow (high-efficiency heat and mass transfer when static mixing is introduced) with high throughput of the cooling crystallisation operation. A COBC unit is a tubular crystalliser with regularly spaced internal baffles, which facilitate static mixing by subjecting the multicomponent fluid stream to oscillatory flow (overall, material still flows in one direction) (Lawton et al., 2009).

Despite their recent introduction in regard to commercial availability, COBC units are reported to offer excellent control for cooling crystallisation due to their high specific surface areas (compared to stirred tanks), and efficient scalability which can be ensured by monitoring the dimensionless numbers that describe the underlying heat, mass and momentum transport phenomena underlying the continuous crystallisation process in COBC systems (McGlone et al., 2015).

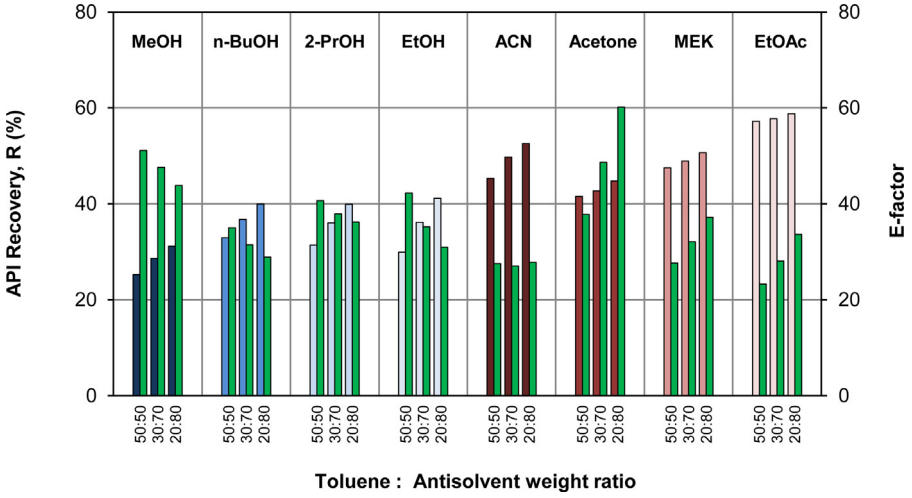

Fig. 7. Continuous crystallisation: simulated candidate antisolvent performance (Jolliffe and Gerogiorgis, 2016b).

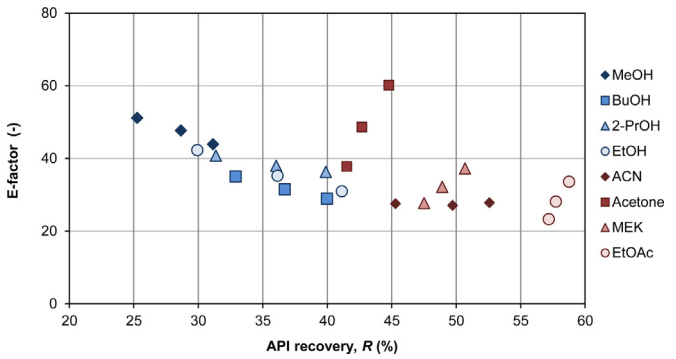

Fig. 8. Environmental impact of continuous crystallisation (lower *E*-factors are superior) as a function of API recovery: simulated candidate antisolvent performance (Jolliffe and Gerogiorgis, 2016b).

3. Nonlinear optimisation problem formulation

The total cost minimisation problem is formally posed as a sum of capital as well as time-discounted operating expenditure:

$$\min Cost_{Tot} = CapEx + \sum_{t=1}^{\tau} \left\{ \frac{OpEx}{(1+y)^t} \right\} \tag{1}$$

s.t.

$$CapEx = BLIC + \gamma_{cont} + \gamma_{wc} \tag{2}$$

$$OpEx = \gamma_{mat} + \gamma_{energy} + \gamma_{utl} + \gamma_{was} \tag{3}$$

$$100\text{kg yr}^{-1} \leq \dot{m}_{API,prod} \tag{4}$$

$$5^{\circ}\text{C} \leq T_{Crys,LO} \leq 39^{\circ}\text{C} \tag{5}$$

$$0.5 \leq m_{Crys,AS} \leq 0.8 \tag{6}$$

The total CPM process cost is hence calculated by considering all individual contributions to Capital Expenditure (*CapEx*) and Operating Expenditure (*OpEx*) using Eq. (1), considering all cost items required to purchase, build and run a given design for a specified time period. In this equation τ is the design lifetime (20 years) and y is the discount rate to the present day (5%, i.e. 1.05). The capital expenditure (*CapEx*) consists of the Battery-Limits Installed Cost (*BLIC*), the cost of contingency (γ_{cont}), and working capital (γ_{wc}); the operating expenditure (*OpEx*) consists of material purchase costs (γ_{mat}), energy use costs (γ_{energy}), utilities costs (γ_{util}), and waste disposal costs (γ_{was}).

Key constraints considered in our NLP formulation encompass a target API production of 100 kg year^{-1}, Eq. (4), minimum and maximum crystallisation cooling temperatures, Eq. (5), antisolvent composition ranges, Eq. (6).

3.1. Process modelling

The NLP optimisation formulation includes all necessary equations for PFR reactor sizing, API solubility, and COBC crystalliser design:

$$V_{PFRm} = Q_m C_{mi0} \int_0^{X_{mif}} \frac{dX_{mi}}{-r_{mi}} \tag{7}$$

$$r_{mi} = k_{mi} C_{mi} \tag{8}$$

$$x_{API,Crys} = \alpha_2 T_{Crys}^2 + \alpha_1 T_{Crys} + \alpha_0 \tag{9}$$

$$q_{COBC} = (C_{P,Tol} n_{Tol,COBC} + C_{P,AS} n_{AS,COBC}) \Delta T_{COBC} \tag{10}$$

$$A_{COBC} = \frac{q_{COBC}}{U_{COBC} LMTD_{COBC}} \tag{11}$$

$$\dot{m}_{CW} = \frac{q_{COBC}}{C_{P,CW} LMTD_{COBC}} \tag{12}$$

$$R_{Crys}^T = \frac{(1 - m_{Crys,API,0}) \left(\frac{(\dot{m}_S + \dot{m}_{AS}) m_{Crys,API,0}}{(1 - m_{Crys,API,0})} \right) + \left(\frac{(\dot{m}_S + \dot{m}_{AS}) m_{Crys,API,f}}{(1 - m_{Crys,API,f})} \right)}{(\dot{m}_S + \dot{m}_{AS}) m_{Crys,API,0}} \tag{13}$$

$$R_{Crys} = f_{Crys} R_{Crys}^T \tag{14}$$

PFR reactor volumes (V_{PFRm}) are computed via the standard plug flow reactor performance equation for a first-order reaction in reactor m, using Eq. (7). Here, $\dot{Q}_m$ is the volumetric flowrate through reactor m, subscript i denotes the key reactant species, and C_{mi00} is the initial concentration of key reactant species i in reactor m; X is the reaction conversion, with subscript f denoting the final conversion.

PFR reactor sizing requires explicit knowledge of r_{mi}, which is the reaction rate for key reactant species i in reactor m, and is computed via the standard first-order reaction rate expression, Eq. (8). The reactions for the CPM of artemisinin have been assumed to be first-order given the nature of the reactions (large organic molecules reacting with an excess of smaller reagents, e.g. O_2); data has been available for these reactions, and reaction rate constants have been estimated based on stated conversions and lab-scale reaction line volumes, confirming our reaction order hypotheses:procedural details and results are reported in our recent publications (Jolliffe and Gerogiorgis, 2016a,b,c).

Surrogate equations for API solubility, on the basis of Eq. (9), (Eq. (9) have been derived from our previously computed results (Fig. 5) which have been obtained from extensive UNIFAC simulations (Gracin et al., 2002); these surrogate polynomial functions have been incorporated into the NLP model that we have solved, in order to avoid overcomplicating the nonlinear formulation (including the circumvention of explicit UNIFAC equations in the model, which would induce a significantly increased computational demand). Further details of the UNIFAC-calculated solubilities can be found in our previous publication (Jolliffe and Gerogiorgis, 2016a). The

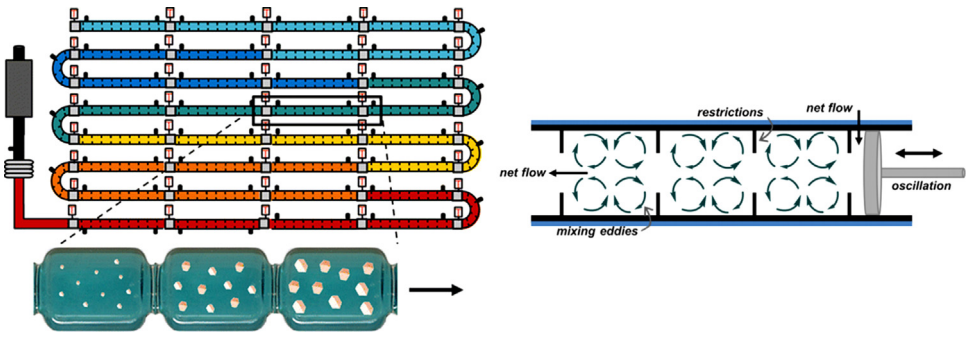

Fig. 9. Continuous Oscillatory Baffled Crystalliser (COBC) configuration (left) and flow pattern (right) (McGlone et al., 2015).

Table 1
Surrogate equation (9) parameters for candidate continuous crystallisation antisolvents at three different mass concentrations.

Antisolvent	Weight percent	Eq. (9) parameter		
		α_2	α_1	α_0
MeOH	50	$1.452 \cdot 10^{-5}$	$1.730 \cdot 10^{-3}$	$8.281 \cdot 10^{-2}$
	70	$1.633 \cdot 10^{-5}$	$1.567 \cdot 10^{-3}$	$6.606 \cdot 10^{-2}$
	80	$1.744 \cdot 10^{-5}$	$1.458 \cdot 10^{-3}$	$5.752 \cdot 10^{-2}$
EtOH	50	$1.617 \cdot 10^{-5}$	$1.465 \cdot 10^{-3}$	$7.538 \cdot 10^{-2}$
	70	$1.832 \cdot 10^{-5}$	$1.247 \cdot 10^{-3}$	$5.564 \cdot 10^{-2}$
	80	$1.984 \cdot 10^{-5}$	$1.068 \cdot 10^{-3}$	$4.430 \cdot 10^{-2}$
PrOH	50	$1.604 \cdot 10^{-5}$	$1.448 \cdot 10^{-3}$	$7.626 \cdot 10^{-2}$
	70	$1.735 \cdot 10^{-5}$	$1.278 \cdot 10^{-3}$	$6.058 \cdot 10^{-2}$
	80	$1.829 \cdot 10^{-5}$	$1.140 \cdot 10^{-3}$	$5.059 \cdot 10^{-2}$
BuOH	50	$1.609 \cdot 10^{-5}$	$1.413 \cdot 10^{-3}$	$7.488 \cdot 10^{-2}$
	70	$1.688 \cdot 10^{-5}$	$1.269 \cdot 10^{-3}$	$6.211 \cdot 10^{-2}$
	80	$1.747 \cdot 10^{-5}$	$1.153 \cdot 10^{-3}$	$5.321 \cdot 10^{-2}$
ACN	50	$1.963 \cdot 10^{-5}$	$1.545 \cdot 10^{-3}$	$4.495 \cdot 10^{-2}$
	70	$2.173 \cdot 10^{-5}$	$1.238 \cdot 10^{-3}$	$3.423 \cdot 10^{-2}$
	80	$2.262 \cdot 10^{-5}$	$1.056 \cdot 10^{-3}$	$2.890 \cdot 10^{-2}$
Acetone	50	$1.623 \cdot 10^{-5}$	$1.585 \cdot 10^{-3}$	$5.471 \cdot 10^{-2}$
	70	$1.709 \cdot 10^{-5}$	$1.487 \cdot 10^{-3}$	$4.991 \cdot 10^{-2}$
	80	$1.811 \cdot 10^{-5}$	$1.408 \cdot 10^{-3}$	$4.519 \cdot 10^{-2}$
MEK	50	$1.804 \cdot 10^{-5}$	$1.458 \cdot 10^{-3}$	$4.564 \cdot 10^{-2}$
	70	$1.875 \cdot 10^{-5}$	$1.353 \cdot 10^{-3}$	$4.169 \cdot 10^{-2}$
	80	$1.956 \cdot 10^{-5}$	$1.271 \cdot 10^{-3}$	$3.822 \cdot 10^{-2}$
EtOAc	50	$2.287 \cdot 10^{-5}$	$1.179 \cdot 10^{-3}$	$3.225 \cdot 10^{-2}$
	70	$2.296 \cdot 10^{-5}$	$1.063 \cdot 10^{-3}$	$3.037 \cdot 10^{-2}$
	80	$2.321 \cdot 10^{-5}$	$9.754 \cdot 10^{-4}$	$2.837 \cdot 10^{-2}$

average R^2 value for surrogate equations used in the present study exceeds 0.99; the parameters obtained for Eq. (9) are tabulated in Table 1, corresponding to solubility curves at 50, 70 and 80% of weight-based antisolvent concentration (in reference to the solute-free solution in the crystallisation). Quadratic interpolation has been performed as required, in order to obtain the API solubility curves for weight percentages between the foregoing antisolvent mass concentration values.

The energy requirement for cooling the COBC crystallisation units (q_{COBC}) has been computed via a standard homogeneous heat transfer equation, which considers the operating temperature change and the multicomponent mixture heat capacity (Eq. (10)). This is then used in order to determine the required internal surface area for heat transfer (A_{COBC}, Eq. (11)). Therein, U_{COBC} is the overall heat transfer coefficient, assumed at a conservative value of 100 $W\,m^{-2}\,K^{-1}$. Moreover, LMTD is the logarithmic mean temperature difference. The cooling medium (brine) requirement is similarly computed via Eq. (12), where $C_{P,CW}$ is the heat capacity of the brine.

The theoretically achievable API product recovery (R^T_{Crys}) is calculated from the API mole fraction solubility ($m_{Crys,API}$, Eq. (13)), which is in turn computed from the corresponding parameterisation of surrogate API solubility Eq. (9). Further key NLP optimisation decision variables here are the mass of solvent (m_S) and antisolvent (m_{AS}) in the crystallisation unit operation(s). The actual API recovery is then computed from R^T_{Crys} by applying a factor (f_{Crys}, as per Eq. (14)) which accounts for the difference between attainable mass transfer in regard to thermodynamic equilibrium, due to the inevitably limited residence time implied by continuous crystallisation; this crystallisation efficiency factor has been assumed at the conservative value of 70%.

3.2. Cost estimation

The total CPM process cost minimisation model assumes an 8040-hour (335-day) working year, for a design to be constructed at an existing pharmaceutical facility. Both the Capital Expenditure (*CapEx*) and the Operating Expenditure (*OpEx*) have been estimated using publicly available commercial vendor data and established cost estimation methods. Equipment vendor prices have been used for process equipment if data for similar capacity is available, and capacity-cost correlations have been used whenever such data is unavailable (Woods, 2007).

$$BLIC = FOB_{tot}\,\gamma_{ins}(1 + \gamma_{pip} + \gamma_{ins2})(1 + \gamma_{ec}) \tag{15}$$

$$FOB_{Tot} = \sum_i f_{\gamma i} n_i \gamma_{ai} \left(\frac{S_{bi}}{S_{ai}}\right)^{p_i} \tag{16}$$

$$\gamma_{cont} = f_{con} BLIC \tag{17}$$

$$\gamma_{wc} = f_{wc}\gamma_{mat} \tag{18}$$

$$\gamma_{mat} = \sum_j R_j \pi_j \tag{19}$$

$$\gamma_{utl} = f_{utl} \sum_j R_j \tag{20}$$

$$\gamma_{was} = f_{was}\dot{v}_{was} \tag{21}$$

The Capital Expenditure, *CapEx*, (2), is computed via Eq. (2) and includes the Battery Limits Installed Cost (*BLIC*), the contingency (γ_{cont}) and the working capital (γ_{wc}). Reference and design values for equipment are denoted by subscripts *a* and *b*, respectively. Equipment capacities are denoted by *S*. These capacities are of a dimension inherent to the equipment in question, such as volume for a reactor, and internal area for the COBC unit. The empirical exponent *p* varies by equipment, and ranges between 0.1–1.0; moreover, other factors (summarised in the multiplier $f_{\gamma i}$) have been used to account for design options (such as operating conditions or construction material). The Chemical Engineering Plant Cost Index (CEPCI) has been used to calculate the appropriate inflation adjustments for equipment prices as necessary, depending on data availability.

Adjusting Eq. (16) for inflation produces the free-on-board (*FOB*) cost. The battery-limits-installed-cBattery Limits Installed Cost (*BLIC*) is then estimated via the Chilton method (Couper, 2003), with the following factors used: the installed equipment cost (γ_{ins}) is 1.43 times the *FOB*, while the process piping (γ_{pip}) and instrumentation (γ_{ins22}) costs are 0.3 and 0.12 times the installed equipment costs, respectively. The total physical plant cost is the sum of the installed, piping, and instrumentation costs, and a final factor for engineering and construction (γ_{ec}, with a value of 0.3) has been applied in order to compute the *BLIC* value. The working capital cost (γ_{wc}) has been assumed at 3.5% of annual material costs (γ_{mat}), and the contingency cost (γ_{cont}) has been set at 20% of the *BLIC* value (Schaber et al., 2011). Finally, the total *CapEx* required is the sum of the *BLIC*, the working capital cost and the contingency cost, from Eq. (2).

The Operating Expenditure (*OpEx*) encompasses the appreciable cost of material purchase (γ_{mat}) –, which includes raw materials, process solvent and separation antisolvent, and is calculated using Eq. (3). Material prices have been sourced from vendors and official records of imports and exports to and from a wide range of countries. The balance includes costs for utilities (γ_{utl}) and waste disposal (γ_{was}), which have been estimated using a subset of the heuristics employed by Schaber et al. (2011). Utilities costs are estimated on the basis of total material input, with a figure of £0.96 kg^{-1} used. The vast majority of waste is solvent and antisolvent, hence

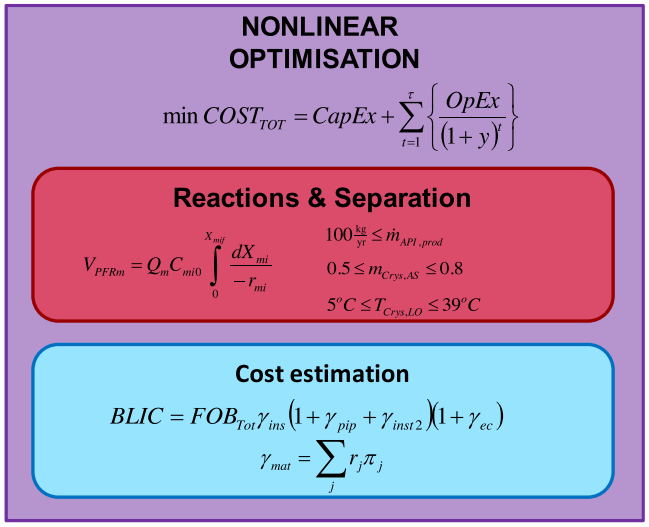

Fig. 10. Illustrative overview of NLP code structure for continuous artemisinin crystallisation (implemented in MATLAB®).

the respective compounds are the only ones considered in order to calculate waste handling costs (taken as £0.35 L^{-1}).

3.3. Constraints

The NLP optimisation model has been implemented in MATLAB®, addressing the total process cost minimisation: each combination of considered antisolvent and number of crystallisers (n_{COBC}) has been separately considered, in order to avoid the need for mixed-integer (MI) formulations and preserve its conciseness.

$$1 \le n_{COBC} \le 5 \tag{22}$$

$$0 \le x_{ki} \le 1 \forall \quad k, i \tag{23}$$

$$\sum_i x_{ki} = 1 \tag{24}$$

The main decision variables are the cooling temperature which is essential for crystalliser operation, according to Eq. (5), and the antisolvent weight concentration in the crystallisation liquid mixture, as per Eq. (6). The decision variables have been constrained within the range from which the surrogate equations have been derived (between 5 and 39 °C for crystallisation cooling temperature, and between 50% and 80% for antisolvent weight concentration, respectively). The use of multiple crystallisers in series has also been studied in order to evaluate the potential for higher API recovery: crystallisers of either fixed or variable (at each step) volume have been considered. A maximum of five crystallisers has been imposed, Eq. (22). A separate NLP optimisation problem instance has been solved for each case, in order to avoid MI programming formulations. The essential molar fraction constraints of Eq. (23) and (24) have also been included in the NLP formulation.

3.4. NLP optimisation: code structure and subroutines

The NLP optimisation code has been structured in three distinct portions; a section implementing reactions and reactor sizing, thermodynamics and product recovery equations; a section implementing cost estimation equations; and a section implementing the NLP optimisation problem itself. An NLP code architecture diagram is given in Fig. 10.

The MATLAB® fmincon solver has been employed, using the available trust-region-reflective method with automatic gradient calculation. The solver has been initialised from a broad, equispaced grid of starting points corresponding to numerous design variable combinations, in order to ensure that the optimal solution is unique in each NLP problem instance, and independent of initialisation. This initialisation grid consists of all possible (25) combinations of antisolvent mass concentration ($x_{Crys,AS,0}$, between 55% and 75% wt., at increments of 5%) and crystallisation cooling temperature ($T_{Crys,LO,0}$, between 10 °C and 30 °C, at increments of 5 °C). Furthermore, the visualisation of the entire objective function (total cost) surface for all antisolvents confirms that no multiple optima should be expected, due to its confirmed and consistent convexity.

4. Results and discussion

The minimum optimal cost when considering only one crystalliser has been obtained for acetonitrile (ACN) at 80% wt. and cooled to 5 °C, and is equal to $761{\cdot}10^3$ GBP. The total cost surfaces are presented in Fig. 11 in order of increasing optimal cost from the top to the bottom of the left, and then the right column (this is the order of ascending total cost surface minima, which are at the lowest point of each 3D colourmap). Acetonitrile (ACN) is the most promising antisolvent because it induces the minimum total cost, while butanol (BuOH) is the least preferable one, since it incurs the highest total cost).

4.1. Effect of temperature, antisolvent selection and concentration

The most decisive determinant of total process cost is the cooling temperature of continuous artemisinin crystallisation: despite the cooling cost contribution to *OpEx*, efficient cooling and lower COBC temperatures positively affect the required *CapEx*, because they allow for smaller and cheaper COBC crystallisers, as well as higher API recovery, which thereby requires a less expensive plant in order to meet the target API production capacity (100 kg yr^{-1}). Fig. 11 presents the total cost surfaces obtained for the case of a single COBC crystalliser and all eight candidate antisolvents; the horizontal COBC cooling temperature axis has been restricted to a maximum value of 25 °C, so as to to allow for a better visualisation of the trends at the lower temperature end(crystallisation cooling temperatures above 25 °C are not technically promising, because the total cost increases very rapidly).

These total cost surfaces for continuous crystallisation feature considerable variability and certain ones intersect when superimposed, but the most important and universal observation is that they are consistently convex for all eight candidate antisolvents: consequently, the global total cost minimum is attained for the lowest cooling temperature and the highest antisolvent mass concentration which is technically attainable. Methanol performs very poorly under limited cooling (high COBC temperature), but remains more preferable in comparison to propanol and butanol in terms of optimal cost (that is, when operating under high cooling and higher antisolvent mass concentration). This is intuitively expectable, because candidate antisolvents have different responses of API solubility to temperature. The antisolvents studied here as well as previously (Jolliffe and Gerogiorgis, 2016b) have been identified from a Pfizer solvent selection guide (Alfonsi et al., 2008).All but one have been listed therein as 'preferred' substances: seven of the eight feature the expected combination of process efficiency, safety, environmental impact, toxicity, and other associated criteria, with the exception of acetonitrile, which is marginally less desirable but still classified as 'usable' (Alfonsi et al., 2008). While a wider spectrum of candidate antisolventscan potentially offer improved performance over the eight ones studied here, liquid substances which are highly harmful or dangerous (either to human health and safety or to the environment) have not been considered.

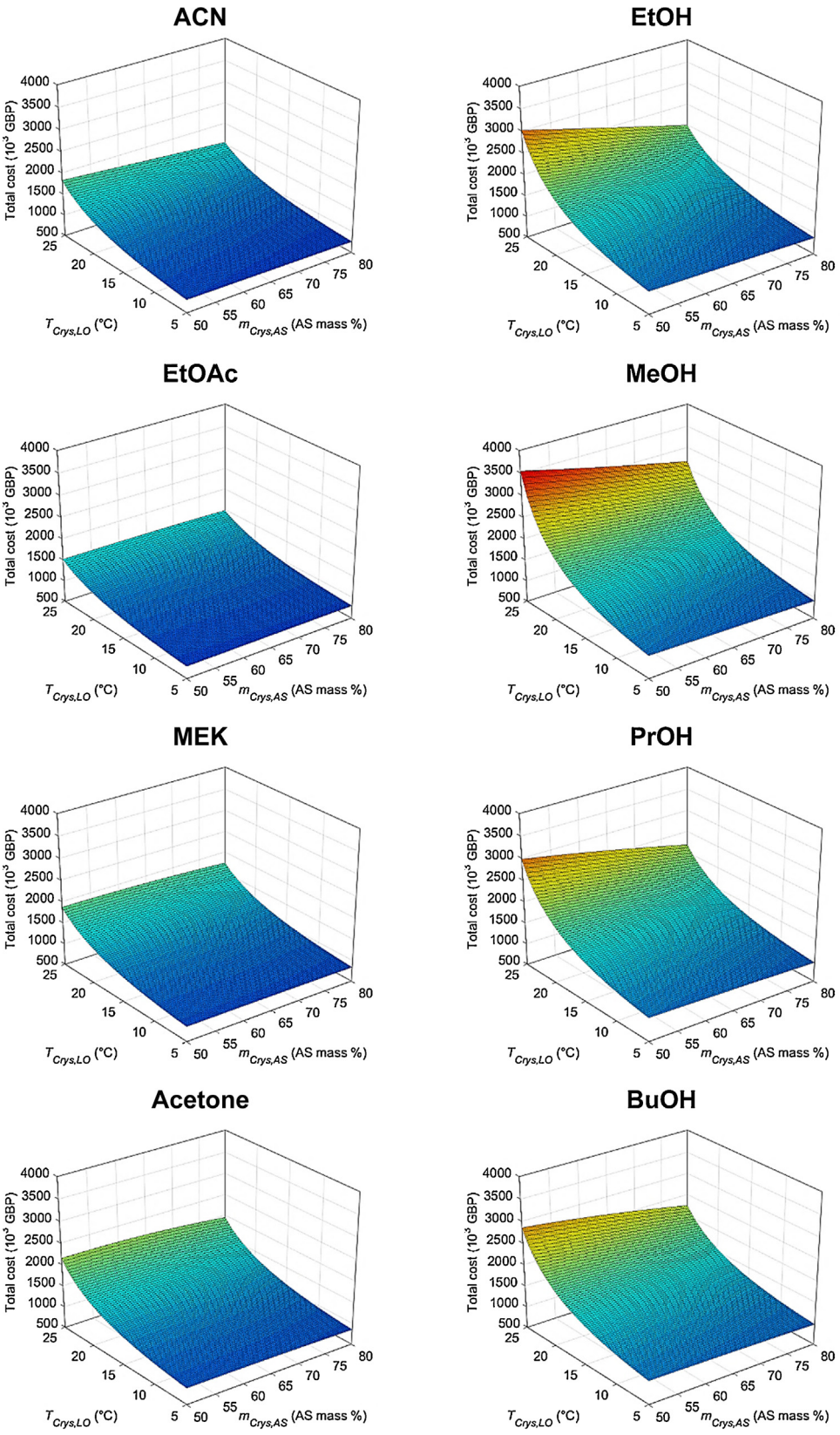

Fig. 11. Total cost surfaces for a single continuous artemisinin COBC crystalliser, in ascending minimum cost order.

The effect of antisolvent concentration on total process cost is less pronounced than that of cooling temperature, but it is nevertheless significant. While the impact is more evident in Fig. 1 for those antisolvents which induce the highest total costs, it is clear that higher rates of antisolvent use favourably reduce total continuous crystallisation costs. An essential clarification is that the total multicomponent content of the crystalliser remains the same, and it is merely the proportion of raw feed solvent (toluene) to antisol-

vent that changes. Moreover, the total continuous crystallisation cost reduction is a decreasing function of antisolvent mass concentration, but at universally smaller (or even barely observable) slopes in comparison to cooling temperature dependence, for all candidate antisolvents. There is an evident theoretical limit to this potential (albeit marginal) improvement, but antisolvent addition can only be performed at finite rates: the best feasible CPM design choice for commercial implementation must also consider the need for complete solvent removal and for prevention of concurrent impurity precipitation (Horváth et al., 2015).

4.2. Multiple crystallisers: effect on economics and environmental impact

The potential use of multiple COBC crystallisers in series has also been investigated as part of this technoeconomic optimisation study (Table 2, Fig. 12). Commercial crystallisation implementations (including current batch pharmaceutical production processes) commonly use multiple crystallisers: it is in fact rather uncommon for a single crystalliser to suffice in order to simultaneously meet the stringent requirements of high product purity, high overall yield, and acceptable cost. The present study considers an operation in which the mother liquor from a crystalliser can be concentrated, so that another crystallisation can be subsequently performed. Two different possibilities have been considered: in the first, all COBC crystallisers have the same size; in the second, the COBC crystallisers can be of variable size. Fig. 9 clearly indicates that there is a significant benefit when using a second crystalliser for seven out of the eight candidate antisolvents, and for both fixed and variable sizes (naturally, when there is only one crystalliser, the costs are the same for both fixed and variable size). The only notable exception is acetonitrile (ACN), for which the API recovery is such that the use of two crystallisers of the same size induces a total cost which is higher than the case of employing just one; however, for crystallisers of variable size, two crystallisation units are optimal for acetonitrile (ACN). Employing COBC crystallisers of variable size may seem an obvious and intuitive design objective, but our purpose here is the precise and comparative evaluation of projected benefits for all antisolvents, COBC sizes and operational configurations. The expected benefit computed on the basis of our NLP optimisation model for continuous artemisinin crystallisation is in the order of $50 \cdot 10^3$ GBP; accordingly, there is a strong incentive to use COBC units of variable size, in comparison to the respective crystallisers of fixed size.

The *E*-factor, first used by Sheldon (2012), is a versatile and useful green chemistry metric. The simplest definition of the *E*-factor is the quantity of waste generated per unit mass of product: values as high as 200 are common for pharmaceutical processes, which are predominantly batch operations; conversely, highly efficient industries which rely on continuous production methods (such as oil and gas extraction and refining) enjoy remarkably low *E*-factors in the order of 0.1, indicating extremely high mass efficiency and consequently very low waste generation (Ritter, 2013). The present study employs the foregoing *E*-factor definition according to Eq. (25), in which the environmental impact metric is computed on the basis of pure recovered API product, while the waste consists of byproducts (BPD), unconverted reactants (UR), waste solvent (WS, 10% of the total quantity has been assumed unrecoverable), waste antisolvent (WAS, all assumed unrecoverable) and unrecovered API (*UAPI*):

$$E\text{-factor} = \frac{m_{Waste}}{m_{API}} = \frac{m_{BPD} + m_{UR} + m_{WS} + m_{WAS} + m_{UAPI}}{m_{API}} \tag{25}$$

The *E*-factorhas not been included as an explicit objective term or constraint in the NLP optimisation problem formulation. The respective values for all continuous crystallisation cases and COBC configurations have been computed in order to gain a more detailed understanding of the optimised costs, so as to further evaluate the interplay between process efficiency, economic viability and environmental impact of this (and similar) conceptual CPM processes.

The *E*-factor continues to improve when using more crystallisers of variable size, at least up to the upper bound (5) considered here, in contrast to the respective total process cost trend (Fig. 11). For a single crystalliser, the use of butanol results in the highest *E*-factor, and the use of acetonitrile in the lowest. The order for the *E*-factors here (for one crystalliser) is identical to the order of total costs. This order changes with the use of more crystallisers: when using four or five crystallisers of fixed size, ethanol (not butanol) has the highest and least attractive *E*-factor. For some antisolvents, most apparently for ethyl acetate, *E*-factors for a series of fixed-size crystallisers begin to increase for four or more crystallisers; this effect is due to the relatively greater quantities of antisolvent required for the amount of API recovered (Fig. 13).

The general improvement in *E*-factor (the decreasing trend evident in Fig. 13 due to the use of more crystallisers) is achieved because of increasing plantwide API product recovery efficiency, according to Eq. (25). An increased number of crystallisers enables additional (secondary, tertiary, quaternary or even quinary) API product recovery, thereby reducing the numerator and simultaneously increasing the denominator in the *E*-factor definition. The biggest improvement is achieved when expanding from one to two COBC crystallisers, and each further expansion incurs a less significant improvementwhich therefore limits the scope of increasing the continuous separation plant size: the increase in total cost from two to three (or more) crystallisers is unlikely to be justified by additional incremental *E*-factor improvements, as the latter are not combined with appreciable efficiency improvements.

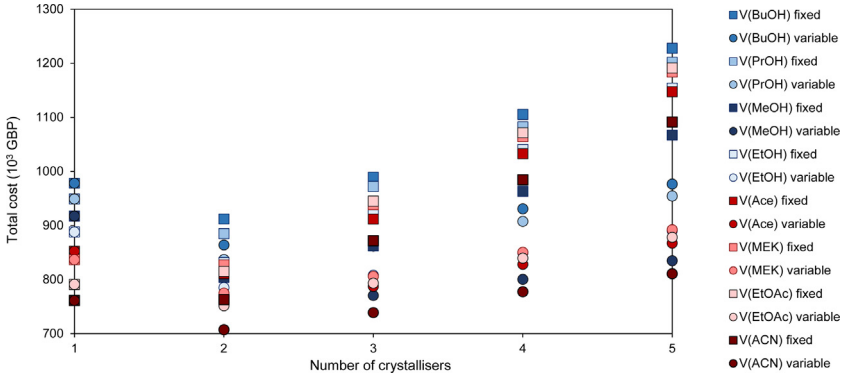

Fig. 12. Optimal total costs for multiple COBC crystallisers (squares: fixed volume crystallisers; circles: variable volume crystallisers).

Table 2
Key NLP optimisation results for total process cost and environmental impact (*E*-factor).

Antisolvent	Optimal total cost (10^3 GBP)		Fig. 11, max (10^3 GBP)	API recovery (%)	*E*-factor (min)
	1 crystalliser	2 crystallisers[a]			1 (5) crystallisers
ACN	761	707	1824	58.08	29.1 (17.6)
EtOAc	791	751	1508	58.05	29.6 (18.1)
MEK	837	775	1866	53.76	32.6 (17.9)
Acetone	852	762	2146	50.52	33.9 (18.4)
EtOH	888	785	3016	35.31	35.3 (18.4)
MeOH	917	768	3546	43.95	37.7 (17.8)
PrOH	949	837	2977	45.51	37.9 (19.3)
BuOH	978	862[b]	2851	44.40	39.5 (19.2)

[a] Optimal number of crystallisers.
[b] 3 crystallisers is optimal for BuOH.

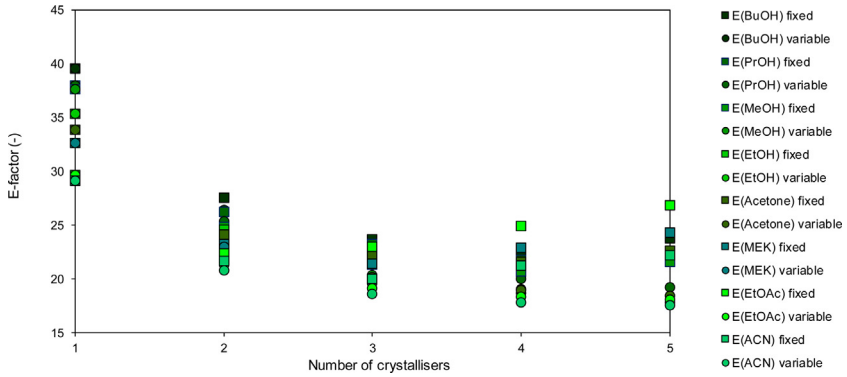

Fig. 13. Environmental impact: *E*-factors for multiple COBC crystallisers (squares: fixed volume crystallisers; circles: variable volume crystallisers).

4.3. Crystalliser size

The required COBC crystalliser volumes vary significantly as a function of the candidate antisolvent and the maximum number of equipment units allowed, as can be seen in Fig. 11: although the COBC crystalliser volume trend does not exactly follow the order of total costs, there are remarkable observations: butanol (BuOH) is the least preferable antisolvent, because it incurs the highest total cost minimum and requires the largest COBC crystalliser volume for a single equipment unit. Acetonitrile (ACN) is the most preferable antisolvent, because it achieves the lowest total cost minimum, as a result of the second lowest COBC crystalliser volume required. The differences arise from the thermodynamic characteristics of the antisolvents, which determine cooling requirements and costs. With the use of more crystallisers, COBC unit sizes decrease: for a given antisolvent, the size of crystalliser number n in the series is smaller when more crystallisers are being used overall. Moreover, the decrease in COBC size is greatest initially, when moving from one to two crystallisers, and this is clearly reflected in total cost trends: indeed, for more than two COBC crystallisers in series, the total cost increases, rendering any further expansion economically disadvantageous.

For a single crystalliser, there is obviously no difference in using fixed or variable size COBC crystallisation units. In several of the antisolvent/number of crystalliser cases considered, the size of the fixed crystalliser is very similar to the first in the corresponding series of variable-volume crystallisers (e.g. the alcohols, two crystallisers). For other cases (three or more crystallisers), the fixed-sized COBC units are smaller than the first, but larger than the subsequent variable-volume crystallisers.

The sizes of COBC crystallisers are determined on the basis of heat transfer requirements, given the extreme scarcity of crystal growth kinetics for the API-solvent-antisolvent systems considered here; their computational determination also relies on corresponding lab-scale batch crystallisers (Horváth et al., 2015). For commercial implementation, there are important considerations for crystal size distribution and morphology, which are strictly specified by pharmaceutical product regulations (Desiraju and Nangia, 2016). For further design and analysis towards industrial implementation, comprehensive experiments elucidating artemisinin crystal growth kinetics and mechanisms are required (Malwade et al., 2013, 2016). The use of COBC units promises significant benefits, as it has been reported to offer excellent control over crystal formation and growth (McGlone et al., 2015) (Fig. 14).

By the fifth crystalliser, the quantities of material processed are very small, leading to low heat transfer requirements and small volumes. Notwithstanding the likely design hurdles in operating COBC crystallisation units at this size, the clear conclusion is that the optimal cost in most cases is achieved for no more than two COBC crystallisers. The optimal choiceis therefore to use acetonitrile (ACN) or ethyl acetate (EtOAc), to mitigate environmental impact, as antisolvent, and a system of twoCOBC crystallisers in series of sequentially decreasing size, operating at a crystallisation cooling temperature of 5 °C, with the use of an 80% antisolvent (acetonitrile) mass concentration (solute-free basis).

4.4. Maintenance and operability considerations

Maintenance and operability are crucial considerations in order to ensure a rapid and smooth transition from the conceptual and laboratory process R&D stages to commercial implementation. While continuous manufacturing requires less cleaning than batch operations (due in large part to the inherent requirements of batch processing, as well as its multi-purpose nature) and can operate for long periods without scheduled maintenance shutdowns, continuous processing equipment tends to be more complex than the respective batch processing units. Furthermore, the construction, installation, operation and maintenance of COBC crystalliser units

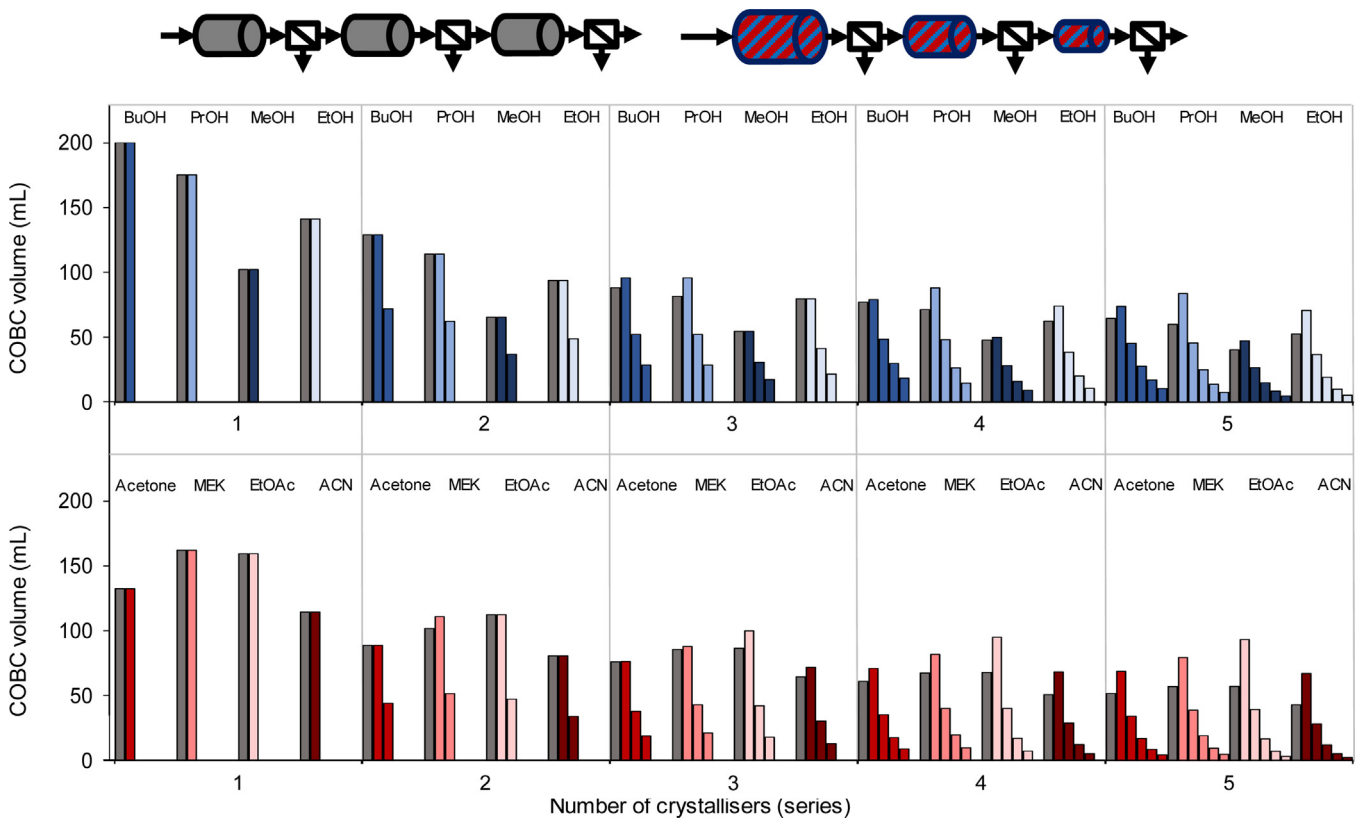

Fig. 14. Optimal COBC crystalliser volumes; grey columns indicate a series of COBCs of identical volumes, coloured bars indicate a series of COBCs of varying volumes. (For interpretation of the references to colour in this figure legend, the reader is referred to the web version of this article.)

of very small volume and/or internal diameter may be prohibitively impractical for commercial implementation - this is a point which illustrates that technical efficiency and economic viability is scale-dependent, and a strong function of plant capacity. Consequently, maintenance and operability costs and their variation between single and multiple crystallisers, and between multiple crystallisers of fixed volume (equally sized crystallisers in series) and variable volume (crystallisers in series of sequentially decreasing volume) are essential in order to further elaborate on the comparative technoeconomic evaluation of potential continuous COBC crystallisation versus batch crystallisation implementations.. While COBC crystallisation units rely on plug flow theirbaffles and oscillating flow pattern are reliable safeguards against potential blockage.

4.5. *Wider applicability of employed methods*

The present study employs a wide spectrum of established process systems engineering methods, including kinetic parameter and thermophysical property estimation, estimation of API solubilities via group contribution (UNIFAC) methods, and most importantly economic evaluation and environmental impact assessment within the framework of a nonlinear optimisation problem, towards achieving total cost minimisation for a continuous pharmaceutical process. Traditionally, batch operation is vastly more prevalent in the pharmaceutical industry. The methods and framework used here could be adapted for a batch process instead, and methods used in the present study have indeed been employed in technoeconomic evaluations of both batch and continuous processes (Schaber et al., 2011; Heider et al., 2014; Ott et al., 2016). To extend the current systematic NLP optimisation methodology for implementation in a respective batch process, the presented formulation would have to be significantly augmented: the resulting model must encompass all technical features of the respective unit operations, but most importantly the operational aspects of production vs. maintenance and idle time, in order to ensure a fully elucidated (hence fair) comparison, on a realistic and suitably justified basis.

5. Conclusions

The present paper presents the detailed technoeconomic process modelling and investigation of eight candidate antisolvents for the systematic optimisation of continuous artemisinin recovery via cooling COBC crystallisation. The NLP problem formulation addresses total cost minimisation for a 20-year design lifetime, and simultaneously explores process mass efficiency and environmental impact, which is evaluated in terms of *E*-factor (a widely used green chemistry metric). Key process decision variables are the continuous crystallisation cooling temperature, and the nature and mass concentration of the crystallisation antisolvent; the use of multiple crystallisers in series has been also investigated in order to elucidate the potential for total cost and mass efficiency improvements.

Eight antisolvents have been identified and studied here, on the basis of a solvent selection guide published recently (Alfonsi et al., 2008). Acetonitrile presents the best continuous crystallisation option, achieving the lowest minimum total cost for one crystalliser out of all candidate antisolvents ($761 \cdot 10^3$ GBP, for a crystallisation at 5 °C, with 80% antisolvent addition and an *E*-factor of 29.1). The use of additional COBC crystallisers in series allows an improvement in total cost: this occurs up to the use of two crystallisers for all antisolvents except one (namely butanol, for which the minimum total cost is achieved for three crystallisers), while *E*-factors continue to improve, albeit with diminishing returns as the total number of COBC crystallisers increases. The computed optimal COBC crystalliser volumes are heavily influenced by the

heat transfer requirements: each successive COBC crystalliser is consistently smaller than the previous one when variable size is allowed, for all candidate solvents and all COBC configurations studied. The formulation and solution of an NLP optimisation model for total continuous COBC crystallisation cost minimisation illustrates how the implementation of established process systems engineering methodologies can catalyse the development of novel CPM flowsheets and plants, with simultaneous consideration and quantification of critical performance characteristics (such as the environmental impact, here monitored via the *E*-factor) towards determining and constructing optimised CPM solutions of superior technical performance and guaranteed economic viability.

Acknowledgments

The authors gratefully acknowledge the financial support of the Engineering and Physical Sciences Research Council (EPSRC) via a Doctoral Training Partnership (DTP) studentship awarded to Mr H.G. Jolliffe. Tabulated and cited literature data suffice for reproduction of all original process simulation and optimisation results, and no other supporting data are required to ensure reproducibility.

References

Abejón, R., Garea, A., Irabien, A., 2014. Analysis and optimization of continuous organic solvent nanofiltration by membrane cascade for pharmaceutical separation. AIChE J. 60, 931–948.

Abejón, R., Garea, A., Irabien, A., 2015. Organic solvent recovery and reuse in pharmaceutical purification processes by nanofiltration membrane cascades. In: Pierucci, S., Klemes, J.J. (Eds.), ICHEAP12: 12th International Conference on Chemical & Process Engineering. Aidic Servizi Srl, Milano, pp. 1057–1062.

Alfonsi, K., Colberg, J., Dunn, P.J., Fevig, T., Jennings, S., Johnson, T.A., Kleine, H.P., Knight, C., Nagy, M.A., Perry, D.A., Stefaniak, M., 2008. Green chemistry tools to influence a medicinal chemistry and research chemistry based organisation. Green Chem. 10, 31–36.

Amara, Z., Bellamy, J.F.B., Horvath, R., Miller, S.J., Beeby, A., Burgard, A., Rossen, K., Poliakoff, M., George, M.W., 2015. Applying green chemistry to the photochemical route to artemisinin. Nat. Chem. 7, 489–495.

Bana, P., Örkényi, R., Lövei, K., Lakó Á, Túrós, G.I., Éles, J., Faigl, F., Greiner, I., 2016. The route from problem to solution in multistep continuous flow synthesis of pharmaceutical compounds. Bioorg. Med. Chem. (in press) http://dx.doi.org/10.1016/j.bmc.2016.12.046.

Boukouvala, F., Ierapetritou, M.G., 2013. Surrogate-based optimization of expensive flowsheet modeling for continuous pharmaceutical manufacturing. J. Pharm. Innov. 8, 131–145.

Couper, J.R., 2003. Process Engineering Economics. Marcel Dekker, Inc.

Desiraju, G.R., Nangia, A., 2016. Use of the term "crystal engineering" in the regulatory and patent literature of pharmaceutical solid forms. Some comments. Cryst. Growth Des. 16, 5585–5587.

Diab, S., Gerogiorgis, D.I., 2017. 2017. Process modelling, simulation and technoeconomic evaluation of separation solvents for the Continuous Pharmaceutical Manufacturing (CPM) of diphenhydramine. Org. Process Res. Dev., http://dx.doi.org/10.1021/acs.oprd.6b00386 (in press).

EFPIA, 2013. The Pharmaceutical Industry in Figures - Key Data 2013 [WWW Document] (accessed 31/1/2014) URL http://www.efpia.eu/uploads/Figures_Key_Data_2013.pdf.

Escotet-Espinoza, M.S., Rogers, A., Ierapetritou, M., 2016. Optimization methodologies for the production of pharmaceutical products. In: Ierapetritou, M.G., Ramachandran, R. (Eds.), Process Simulation and Data Modeling in Solid Oral Drug Development and Manufacture, Methods in Pharmacology and Toxicology. Springer, New York, pp. 281–309.

Gernaey, K.V., Cervera-Padrell, A.E., Woodley, J.M., 2012. A perspective on PSE in pharmaceutical process development and innovation. Comput. Chem. Eng. 42, 15–29.

Gerogiorgis, D.I., Barton, P.I., 2009. Steady-state optimization of a continuous pharmaceutical process. In: de Brito Alves, Rita Maria, C.A.O. do N, ECB (Eds.), Computer Aided Chemical Engineering, 10th International Symposium on Process Systems Engineering: Part A. Elsevier, pp. 927–932.

Gilmore, K., Kopetzki, D., Lee, J.W., Horváth, Z., McQuade, D.T., Seidel-Morgenstern, A., Seeberger, P.H., 2014. Continuous synthesis of artemisinin-derived medicines. Chem. Commun 50, 12652–12655.

Gracin, S., Brinck, T., Rasmuson, Å.C., 2002. Prediction of solubility of solid organic compounds in solvents by UNIFAC. Ind. Eng. Chem. Res. 41, 5114–5124.

Grom, M., Stavber, G., Drnovšek, P., Likozar, B., 2016. Modelling chemical kinetics of a complex reaction network of active pharmaceutical ingredient (API) synthesis with process optimization for benzazepine heterocyclic compound. Chem. Eng. J. 283, 703–716.

Haas, N.T., Ierapetritou, M., Singh, R., 2017. Advanced model predictive feedforward/feedback control of a tablet press. J. Pharm. Innov., 1–14.

Heider, P.L., Born, S.C., Basak, S., Benyahia, B., Lakerveld, R., Zhang, H., Hogan, R., Buchbinder, L., Wolfe, A., Mascia, S., Evans, J.M.B., Jamison, T.F., Jensen, K.F., 2014. Development of a multi-step synthesis and workup sequence for an integrated, continuous manufacturing process of a pharmaceutical. Org. Process Res. Dev. 18, 402–409.

Horváth, Z., Horosanskaia, E., Lee, J.W., Lorenz, H., Gilmore, K., Seeberger, P.H., Seidel-Morgenstern, A., 2015. Recovery of artemisinin from a complex reaction mixture using continuous chromatography and crystallization. Org. Process Res. Dev. 19, 624–634.

Ierapetritou, M., Muzzio, F., Reklaitis, G., 2016. Perspectives on the continuous manufacturing of powder-based pharmaceutical processes. AIChE J. 62, 1846–1862.

Jensen, K.F., 2017. Flow chemistry—microreaction technology comes of age. AIChE J. 63, 858–869.

Jolliffe, H.G., Gerogiorgis, D.I., 2016a. Process modelling and simulation for continuous pharmaceutical manufacturing of artemisinin. Chem. Eng. Res. Des. 112, 310–325.

Jolliffe, H.G., Gerogiorgis, D.I., 2016b. Systematic solvent evaluation for artemisinin recovery in continuous pharmaceutical manufacturing. In: Kravanja, Z. (Ed.), Computer Aided Chemical Engineering. 26th European Symposium on Computer Aided Process Engineering, Elsevier, pp. 1027–1032.

Jolliffe, H.G., Gerogiorgis, D.I., 2016c. Plantwide design and economic evaluation of two Continuous Pharmaceutical Manufacturing (CPM) cases: Ibuprofen and artemisinin. Comput. Chem. Eng. 91, 269–288.

Jolliffe, H.G., Gerogiorgis, D.I., 2017. Technoeconomic optimization of a conceptual flowsheet for continuous separation of an analgaesic Active Pharmaceutical Ingredient (API). Ind. Eng. Chem. Res., http://dx.doi.org/10.1021/acs.iecr.6b02146 (in press).

Kopetzki, D., Lévesque, F., Seeberger, P.H., 2013. A continuous-flow process for the synthesis of artemisinin. Chem. – Eur. J. 19, 5450–5456.

Kralisch, D., Ott, D., Gericke, D., 2014. Rules and benefits of Life Cycle Assessment in green chemical process and synthesis design: a tutorial review. Green Chem. 17, 123–145.

Kwon, J.S.-I., Nayhouse, M., Christofides, P.D., Orkoulas, G., 2014a. Modeling and control of crystal shape in continuous protein crystallization. Chem. Eng. Sci. 107, 47–57.

Kwon, J.S.-I., Nayhouse, M., Orkoulas, G., Christofides, P.D., 2014b. Crystal shape and size control using a plug flow crystallization configuration. Chem. Eng. Sci. 119, 30–39.

Lawton, S., Steele, G., Shering, P., Zhao, L., Laird, I., Ni, X.-W., 2009. Continuous crystallization of pharmaceuticals using a continuous oscillatory baffled crystallizer. Org. Process Res. Dev. 13, 1357–1363.

Lee, S.L., O'Connor, T.F., Yang, X., Cruz, C.N., Chatterjee, S., Madurawe, R.D., Moore, C.M.V., Yu, L.X., Woodcock, J., 2015. Modernizing pharmaceutical manufacturing: from batch to continuous production. J. Pharm. Innov., 1–9.

Malwade, C.R., Buchholz, H., Rong, B.-G., Qu, H., Christensen, L.P., Lorenz, H., Seidel-Morgenstern, A., 2016. Crystallization of artemisinin from chromatography fractions of Artemisia annua extract. Org. Process Res. Dev. 20, 646–652.

Malwade, C.R., Qu, H., Rong, B.-G., Christensen, L.P., 2013. Conceptual process synthesis for recovery of natural products from plants: A case study of artemisinin from Artemisia annua. Ind. Eng. Chem. Res. 52, 7157–7169.

McGlone, T., Briggs, N.E.B., Clark, C.A., Brown, C.J., Sefcik, J., Florence, A.J., 2015. Oscillatory Flow Reactors (OFRs) for continuous manufacturing and crystallization. Org. Process Res. Dev. 19, 1186–1202.

Ott, D., Borukhova, S., Hessel, V., 2016. Life cycle assessment of multi-step rufinamide synthesis – from isolated reactions in batch to continuous microreactor networks. Green Chem. 18, 1096–1116.

Ott, D., Kralisch, D., Denčić, I., Hessel, V., Laribi, Y., Perrichon, P.D., Berguerand, C., Kiwi-Minsker, L., Loeb, P., 2014. Life Cycle Analysis within pharmaceutical process optimization and intensification: Case study of Active Pharmaceutical Ingredient production. Chem. Sus. Chem. 7, 3521–3533.

Paddon, C.J., Westfall, P.J., Pitera, D.J., Benjamin, K., Fisher, K., McPhee, D., Leavell, M.D., Tai, A., Main, A., Eng, D., Polichuk, D.R., Teoh, K.H., Reed, D.W., Treynor, T., Lenihan, J., Jiang, H., Fleck, M., Bajad, S., Dang, G., Dengrove, D., Diola, D., Dorin, G., Ellens, K.W., Fickes, S., Galazzo, J., Gaucher, S.P., Geistlinger, T., Henry, R., Hepp, M., Horning, T., Iqbal, T., Kizer, L., Lieu, B., Melis, D., Moss, N., Regentin, R., Secrest, S., Tsuruta, H., Vazquez, R., Westblade, L.F., Xu, L., Yu, M., Zhang, Y., Zhao, L., Lievense, J., Covello, P.S., Keasling, J.D., Reiling, K.K., Renninger, N.S., Newman, J.D., 2013. High-level semi-synthetic production of the potent antimalarial artemisinin. Nature 496, 528–532.

Patel, M.P., Shah, N., Ashe, R., 2011. Robust optimisation methodology for the process synthesis of continuous technologies. In: Pistikopoulos, E.N., Georgiadis, M.C., Kokossis, A.C. (Eds.), Computer Aided Chemical Engineering, 21st European Symposium on Computer Aided Process Engineering. Elsevier, pp. 351–355.

PATH, 2016. Looking back at 2015. [WWW Document] (accessed 31/8/2016) URL http://sites.path.org/drugdevelopment/2016/01/looking-back-at-2015/.

Ritter, S.K., 2013. Reducing environmental impact of organic synthesis. Chem Eng News, 91.

Rogers, A., Ierapetritou, M., 2015a. Challenges and opportunities in modeling pharmaceutical manufacturing processes. Comput. Chem. Eng. 81, 32–39.

Rogers, A., Ierapetritou, M., 2015b. Feasibility and flexibility analysis of black-box processes. Part 1: surrogate-based feasibility analysis. Chem. Eng. Sci. 137, 986–1004.

Sahlodin, A.M., Barton, P.I., 2015. Optimal campaign continuous manufacturing. Ind. Eng. Chem. Res. 54, 11344–11359.
Schaber, S.D., Gerogiorgis, D.I., Ramachandran, R., Evans, J.M.B., Barton, P.I., Trout, B.L., 2011. Economic analysis of integrated continuous and batch pharmaceutical manufacturing: a case study. Ind. Eng. Chem. Res. 50, 10083–10092.
Seeberger, P.H., Kopetzki, D., Levesque, F., 2014. Method and device for the synthesis of artemisinin, U.S. Patent US20140364630 A1.
Sheldon, R.A., 2012. Fundamentals of green chemistry: efficiency in reaction design. Chem. Soc. Rev. 41, 1437–1451.
Singh, R., Sen, M., Ierapetritou, M., Ramachandran, R., 2015. Integrated moving horizon-based dynamic real-time optimization and hybrid MPC-PID control of a direct compaction continuous tablet manufacturing process. J. Pharm. Innov. 10, 233–253.
Su, Q., Benyahia, B., Nagy, Z.K., Rielly, C.D., 2015. Mathematical modeling, design, and optimization of a multisegment multiaddition plug-flow crystallizer for antisolvent crystallizations. Org. Process Res. Dev. 19, 1859–1870.
Tu, Y., 2011. The discovery of artemisinin (qinghaosu) and gifts from Chinese medicine. Nat. Med. 17, 1217–1220.
Wang, Z., Ierapetritou, M., 2017. A novel feasibility analysis method for black-box processes using a radial basis function adaptive sampling approach. AIChE J. 63, 532–550.
Woods, D.R., 2007. Rules of Thumb in Engineering Practice. Wiley-VCH.